

Chimeric Nature of Pinopsin between Rod and Cone Visual Pigments<sup>†</sup>Atsushi Nakamura,<sup>‡,§</sup> Daisuke Kojima,<sup>‡,§</sup> Hiroo Imai,<sup>§,||</sup> Akihisa Terakita,<sup>§,||</sup> Toshiyuki Okano,<sup>‡,§</sup> Yoshinori Shichida,<sup>§,||</sup> and Yoshitaka Fukada<sup>\*,‡,§</sup>

Department of Biophysics and Biochemistry, Graduate School of Science, The University of Tokyo, Hongo, Bunkyo-Ku, Tokyo 113-0033, Japan, and Department of Biophysics, Graduate School of Science, Kyoto University, Sakyo-ku, Kyoto, 606-8502, Japan

Received June 11, 1999; Revised Manuscript Received August 20, 1999

**ABSTRACT:** Chicken pineal pinopsin is the first example of extra-retinal opsins, but little is known about its molecular properties as compared with retinal rod and cone opsins. For characterization of extra-retinal photon signaling, we have developed an overexpression system providing a sufficient amount of purified pinopsin. The recombinant pinopsin, together with similarly prepared chicken rhodopsin and green-sensitive cone pigment, was subjected to photochemical and biochemical analyses by using low-temperature spectroscopy and the transducin activation assay. At liquid nitrogen temperature (−196 °C), we detected two kinds of photoproducts, bathopinopsin and isopinopsin, having their absorption maxima ( $\lambda_{\text{max}}$ ) at 527 and ~440 nm, respectively, and we observed complete photoreversibility among pinopsin, bathopinopsin, and isopinopsin. A close parallel of the photoreversibility to the rhodopsin system strongly suggests that light absorbed by pinopsin triggers the initial event of *cis-trans* isomerization of the 11-*cis*-retinylidene chromophore. Upon warming, bathopinopsin decayed through a series of photobleaching intermediates: lumipinopsin ( $\lambda_{\text{max}}$  461 nm), metapinopsin I (460 nm), metapinopsin II (385 nm), and metapinopsin III (460 nm). Biochemical and kinetic analyses showed that metapinopsin II is a physiologically important photoproduct activating transducin. Detailed kinetic analyses revealed that the formation of metapinopsin II is as fast as that of a chicken cone pigment, green, but that the decay process of metapinopsin II is as slow as that of the rod pigment, rhodopsin. These results indicate that pinopsin is a new type of pigment with a chimeric nature between rod and cone visual pigments in terms of the thermal behaviors of the meta II intermediate. Such a long-lived active state of pinopsin may play a role in the pineal-specific phototransduction process.

Light signal captured by the chicken pineal gland resets the phase of the endogenous circadian pacemaker (1–4). To understand the pineal phototransduction pathway toward the pacemaker, it is important to investigate molecular properties of the pineal photoreceptive molecules. A variety of photochemical and biochemical studies on retinal visual pigments have successfully explained the difference in physiological photoresponse between rod and cone cells (reviewed in ref 5), but little is known about the molecular properties of photopigments in extra-retinal tissues.

We previously cloned a blue-sensitive pigment, pinopsin, from a chicken pineal cDNA library (6), and it was classified into a novel subtype of the vertebrate rhodopsin family. Interestingly, the phylogenetic analysis showed that pinopsin has diverged from an ancestor of cone pigments before the divergence of rhodopsins from cone pigments (6), suggesting that pinopsin would be a cone-type pigment. If this is the

case, the formation and decay of the meta II intermediate of pinopsin would resemble those of cone pigments, because there is a notable difference in the properties of the meta II intermediate between rod and cone pigments (7–11). Among a series of photobleaching intermediates of visual pigments, the meta II intermediate is identified as a physiologically active intermediate activating a retinal G-protein, transducin (8, 12–14). In this respect, the difference in meta II lifetime has been implicated in cellular responses characteristic of rod and cone cells (5). Therefore, we have focused our interests on the thermal behavior of the meta II intermediate of pinopsin for better understanding of pineal cell physiology.

In the present study, the meta II formation kinetics of pinopsin is shown to be comparable to those of a cone pigment, but its decay profile is very similar to that of rhodopsin. This unique photoreaction of pinopsin is the first example for the chimeric nature between rod and cone type pigments in vertebrates.

## EXPERIMENTAL PROCEDURES

**Buffers.** Buffer P-0 contains 50 mM HEPES<sup>1</sup>–NaOH, 50 kallikrein inhibitor units/mL aprotinin, and 4  $\mu\text{g/mL}$  leupeptin (pH 6.6). Buffers P-10, P-90, P-130, and P-140 are the same

<sup>†</sup> This work was supported in part by Grants-in-Aid from the Japanese Ministry of Education, Science, Sports and Culture.

\* To whom correspondence should be addressed. Tel. and Fax: +81-3-5802-8871. E-mail: sfukada@mail.ecc.u-tokyo.ac.jp.

<sup>‡</sup> The University of Tokyo.

<sup>§</sup> CREST, Japan Science and Technology Corp.

<sup>||</sup> Kyoto University.

as buffer P-0 except for containing 10, 90, 130, and 140 mM NaCl, respectively.

**Expression Constructs and Cells.** Pinopsin cDNA (6) was modified as shown in Figure 1. To introduce six histidine residues and factor Xa site at the N-terminus of pinopsin, first PCR was performed using a pair of primers: 5'-CATCATCACCATCACCACATCGAGGGGCGCATGTC-CTCCAACAGCTCC-3' and 5'-CCCGAATTCACACGGG-GTGTGCTGGC-3'. The PCR product was subjected to the second PCR using another set of primers, 5'-CGGTATCGTC-GATAAGCTTAAACCGCAGCCATGCATCATCACCAC-CACCAC-3' and 5'-CCCGAATTCACACGGGTTGTGCTG-GC-3', to add an 11 bp stretch of chicken rhodopsin 5'-untranslated sequence upstream of the initiation methionine. The resulting amplified product was digested with *Hind*III and *Eco*RI, and subcloned into pBluescript II KS+ (Stratagene). Both strands of the constructed fragments were sequenced to confirm the absence of PCR errors. Similarly, the cDNAs of chicken rhodopsin and green (15) were modified so as to have the same N-terminal tag as described above. To construct opsin expression vectors, each of the modified cDNAs was subcloned into the *Hind*III-*Eco*RI site of mammalian expression vector pUSR $\alpha$  (16), which is a derivative of pUC-SR $\alpha$  (17).

A suspension-adapted variant, 293S (18), of the human embryonic kidney cell line (ATCC CRL 1573) was used as the recipient for transient transfection. The cells were grown in 10% fetal bovine serum, 50:50 DMEM/F12 with low glucose (Gibco) at 37 °C in a 5% CO<sub>2</sub> atmosphere. In a typical experiment, 10  $\mu$ g/plate of the opsin expression vector and 0.5  $\mu$ g/plate of pRSV-TAg (an SV40 T-antigen expression vector) were coprecipitated onto 200, 10 cm diameter plates of 293S cells by the calcium phosphate method (19). Forty hours after transfection, the cells were collected with buffer P-10, and stored at -80 °C until use.

**Reconstitution.** 11-*cis*-Retinal was purified as previously reported (20) and stored at -80 °C until use. The following procedures were performed in the dark or under dim-red light (>660 nm) at 4 °C unless otherwise specified. To generate photopigments, the cells collected as described above were suspended with 25 mL of buffer P-10, and were incubated with an excess amount of 11-*cis*-retinal (about 500 nmol in 250  $\mu$ L of ethanol) for 1 h at room temperature, except for chicken green-expressing cells which were incubated with 11-*cis*-retinal for 4 h at 4 °C. The regenerated photopigment in the suspension was solubilized by mixing with an equal volume (25 mL) of buffer P-10 containing 2% (w/v) dodecyl- $\beta$ -D-maltoside (DM; Dojindo Lab.). The mixture was incubated for 1 h at 4 °C and centrifuged to separate solubilized proteins (termed "cell extract").

**Purification of Pigments.** Pinopsin was purified from the cell extract in the dark or under dim-red light (>660 nm). To increase the relative content of pinopsin, the cell extract was passed through a DEAE-Sepharose column (10  $\times$  38 mm; Amersham Pharmacia Biotech) at a flow rate of 36 mL/h. The flow-through fraction containing most of the solubi-

lized pinopsin was incubated with 2 mL of resin of Probond nickel-charged agarose (Invitrogen) for about 12 h at 4 °C. The resin was packed into a column (10 mm diameter), and washed at a flow rate of 36 mL/h with the following buffers successively: 150 mL of buffer P-140 containing 0.02% DM (w/v) and 50 mL of buffer P-140 containing both 0.02% DM (w/v) and 20 mM imidazole. Then, pinopsin was eluted from the column with 3 mL of buffer P-140 containing both 0.02% DM (w/v) and 200 mM imidazole (pH 6.6). The eluate was dialyzed against buffer P-10 containing 0.02% DM (w/v), and centrifuged at 125000g for 30 min at 4 °C to remove insoluble materials. The clear supernatant containing pinopsin was applied to an SP-Sepharose column (7  $\times$  13 mm; Amersham Pharmacia Biotech) at a flow rate of 18 mL/h. The column was washed with 10 mL of buffer P-10 containing 0.02% DM (w/v), and, then, pinopsin was eluted with buffer P-130 containing 0.02% DM (w/v). The eluate was dialyzed against buffer P-140 containing 0.02% DM (w/v), and used for spectroscopic and biochemical experiments. For low-temperature spectroscopy, the pinopsin solution was concentrated by using Microcon 10 (Amicon), dialyzed, and mixed with a 2-fold or 3-fold volume of glycerol.

Similarly, histidine-tagged chicken green was expressed and purified from the cell extract. In the final step of the SP-Sepharose column chromatography, green was eluted with buffer P-90 containing 0.02% DM (w/v).

Histidine-tagged chicken rhodopsin was expressed and purified from the cell extract with some modifications: To increase the relative content of solubilized rhodopsin, the cell extract was passed through a CM-Sepharose column (Amersham Pharmacia Biotech) instead of the DEAE-Sepharose column. The flow-through fraction containing rhodopsin was similarly purified by the nickel-charged agarose column, and the eluate was dialyzed against buffer P-10 containing 0.02% DM (w/v). After centrifugation, the clear supernatant was dialyzed against buffer P-140 containing 0.02% DM (w/v), and used for spectroscopic and biochemical experiments.

**Spectrophotometry.** The absorption spectra of purified pigments were recorded in a previously reported system (9) with a Shimadzu Model MPS-2000 spectrophotometer interfaced with an NEC PC-9801 computer. An Oxford model CF-1204 cryostat was used for low-temperature spectroscopy. The sample temperature was controlled within  $\pm 0.1$  °C by a temperature controller (ITC-4, Oxford) attached to the cryostat. The sample was irradiated with light from a 1 kW tungsten halogen lamp (Rikagaku Seiki). The wavelength of the irradiation light was selected with a glass cutoff filter (VY-50, VO-54, 59, VR-63; Toshiba), or an interference filter (436 nm; Nihonshinku).

**Transducin Activation Assay.** Transducin was purified from dark-adapted bovine retinas as described elsewhere (21). Transducin activation assays were performed as previously reported (22) with some modifications. Briefly, transducin was mixed with the pigment solution in 50 mM HEPES-NaOH (pH 6.6), 5 mM MgCl<sub>2</sub>, 140 mM NaCl, 1 mM DTT, 0.01% (w/v) DM, and 3  $\mu$ M [<sup>35</sup>S]GTP $\gamma$ S (1500–3000 cpm/pmol) in the dark. After 30 s preincubation, the reaction was started by exposing the mixture containing either pinopsin or rhodopsin to light (>480 nm or >520 nm, respectively) for 30 s at 2 °C, followed by incubation in the dark for 30 s at this temperature. Under the irradiation conditions, the

<sup>1</sup> Abbreviations: HEPES, *N*-(2-hydroxyethyl)piperazine-*N'*-2-ethanesulfonic acid; PCR, polymerase chain reaction; DM, dodecyl- $\beta$ -D-maltoside; GTP $\gamma$ S, guanosine 5'-*O*-(3-thiotriphosphate); DTT, dithiothreitol;  $\lambda_{\text{max}}$ , absorption maximum; CHAPS, 3-[(3-cholamidopropyl)dimethylammonio]-1-propanesulfonate; PC, L- $\alpha$ -phosphatidylcholine from egg yolk.

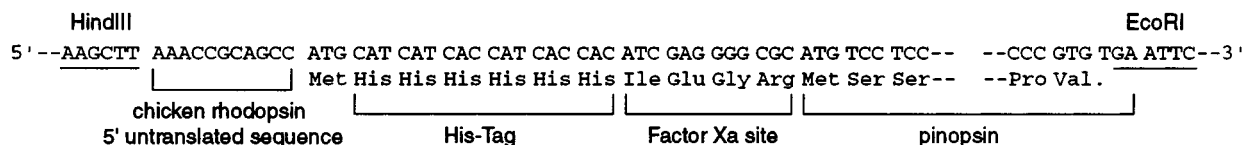


FIGURE 1: Nucleotide sequences at the 5' and 3' ends of the modified pinopsin cDNA. Factor Xa site was introduced for possible removal of the histidine tag after affinity purification, but our several trials failed to cleave the site efficiently. The 5' untranslated sequence of chicken rhodopsin was added for a possible enhancement of pinopsin expression in 293S cells.

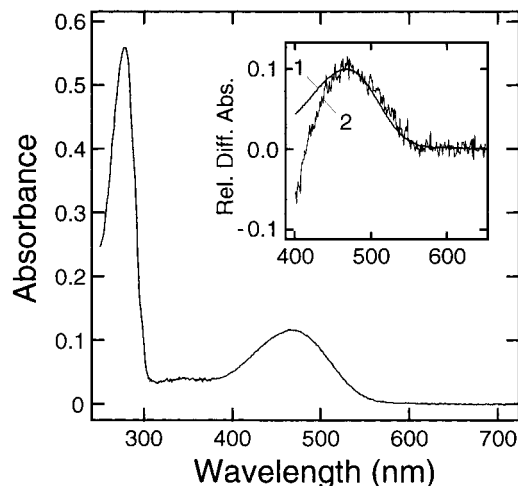


FIGURE 2: Absorption spectra of purified pinopsin. The purified histidine-tagged pinopsin had  $\lambda_{\max}$  at 468 nm, and a typical ratio of  $A_{280}/A_{468}$  was 4.8. (Inset) The absorption spectrum of purified histidine-tagged pinopsin (smooth line; curve 1) is compared with the difference spectrum of nontagged pinopsin before and after complete photobleaching (curve 2, reproduced from ref 6).

pigment in the mixture was completely bleached. The reaction was terminated with a stop solution [20 mM Tris-HCl (pH 7.4), 100 mM NaCl, 25 mM  $MgCl_2$ , and 5  $\mu M$  GTP $\gamma$ S], and the amount of [ $^{35}S$ ]GTP $\gamma$ S bound to transducin  $\alpha$ -subunit was measured as previously reported (21).

## RESULTS

**Purification of Histidine-Tagged Pinopsin.** Pinopsin present in the chicken pineal gland is so small in quantity (23, 24) that an overexpression system in cultured cells is required to obtain a sufficient amount of pinopsin. For affinity purification, the recombinant pinopsin was designed to carry additional six histidine residues at the N-terminus (Figure 1). We avoided tagging at the C-terminus which, in the case of rhodopsin, is exposed to the molecular surface interacting with transducin. The N-terminal tagging was expected to minimize the effect on the signaling properties (see Discussion). The histidine-tagged pinopsin expressed in 293S cells was reconstituted with 11-*cis*-retinal, and solubilized with a detergent, dodecyl- $\beta$ -D-maltoside (DM). The amount of regenerated pinopsin was spectrophotometrically estimated to be about 4  $\mu g/10^7$  cells. Usually 400  $\mu g$  of recombinant pinopsin was obtained from cells cultured in 200, 10 cm plates. Then, pinopsin was purified by three steps of column chromatography (see Experimental Procedures), with a recovery of about 25%. The absorption spectrum of the purified histidine-tagged pinopsin (Figure 2) showed  $\lambda_{\max}$  at 468 nm, which is very close to the  $\lambda_{\max}$  of nontagged pinopsin (about 470 nm in ref 6). Similarly, we prepared modified chicken rhodopsin and green each having a histidine tag at the N-terminus. The recombinant rhodopsin and green

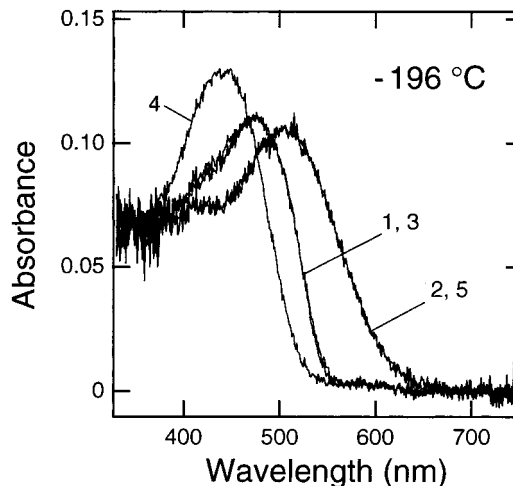


FIGURE 3: Photochemical reactions of pinopsin at liquid nitrogen temperature. Purified chicken pinopsin in 75% (v/v) glycerol mixture was cooled to  $-196^\circ C$  (curve 1) and irradiated with blue light (436 nm) for 1280 s to form a photo-steady-state mixture (curve 2). It was then irradiated with deep-red light ( $>610$  nm) for 240 s (curve 3), followed by irradiation with orange light ( $>560$  nm) for 1920 s (curve 4). This sample was irradiated again with blue light (436 nm) for 640 s (curve 5). In every case, a more prolonged irradiation gave no spectral change, indicating formation of the photo-steady-state mixture.

showed  $\lambda_{\max}$  at 504 and 507 nm, respectively, which were also close to the reported values (25) of native chicken rhodopsin (503 nm) and green (508 nm). Thus, we confirmed that the histidine tag attached to the N-terminus has little effect on the conformation of these pigments, and we used these samples for characterization of pinopsin in comparison with rhodopsin and green.

**Photoreaction of Pinopsin at Liquid Nitrogen Temperature.** Primary photoreactions of pinopsin were investigated by low-temperature spectroscopy. When pinopsin was cooled to  $-196^\circ C$ , its absorption spectrum was sharpened with a slight red-shift of  $\lambda_{\max}$  to 475 nm (Figure 3, curve 1). Irradiation with blue light at this temperature caused a red-shift of the spectrum, indicating the formation of a batho-product (bathopinopsin). Prolonged irradiation finally produced a photo-steady-state mixture containing mainly bathopinopsin (Figure 3, curve 2). Irradiation of the mixture with red light gave a spectrum (curve 3) identical with curve 1. Subsequent irradiation with orange light resulted in formation of a blue-shifted iso-product (curve 4; isopinopsin). This product was irradiated with the blue light, giving a spectrum (curve 5) identical with curve 2. These photoreactions indicate that the original pigment (pinopsin), batho-product, and iso-product were perfectly interconvertible by light at  $-196^\circ C$ , just like retinal visual pigments (9, 11, 26–29).

**Intermediates in the Photobleaching Process of Pinopsin.** In the case of retinal visual pigments, warming of the batho

intermediate results in sequential formation of lumi, meta I, and enzymatically active meta II intermediates (7, 11, 27, 29, 30). To identify the intermediates in the photobleaching process of pinopsin, the photo-steady-state mixture containing mainly bathopinopsin (Figure 3, curve 5) was warmed in a stepwise manner (Figure 4<sup>4</sup>). Bathopinopsin was stable up to  $-190^{\circ}\text{C}$  (Figure 4, curve 2), and the following two intermediates, lumi and meta I, were stable up to  $-70^{\circ}\text{C}$  (curve 11) and  $-50^{\circ}\text{C}$  (curve 13), respectively. As was observed for the bleaching process of chicken blue-sensitive cone pigment (11), we detected a small change in the half-bandwidth without a remarkable shift in the  $\lambda_{\text{max}}$  during the transition from lumi to meta I intermediates (curves 11–13). Above  $-40^{\circ}\text{C}$ , the meta I intermediate was converted to the next meta II intermediate, and its  $\lambda_{\text{max}}$  ( $\sim 380\text{ nm}$ ) was quite similar to those of meta II of retinal visual pigments (7, 9, 11, 29–32). The absorption maxima of the four intermediates were calculated by using a conventional method (9, 33): 527 nm (bathopinopsin), 461 nm (lumipinopsin), 460 nm (metapinopsin I), and 385 nm (metapinopsin II). To sum up, the bleaching process of pinopsin is similar to those observed for visual pigments with respect to the number, the transition temperature of the intermediates, and the transition profile of the absorption maxima (see also Figure 8).

**Formation Process of Metapinopsin II.** Our previous studies revealed that the meta II formation of cone visual pigments is faster than that of rhodopsin (7, 9, 31). To investigate whether pinopsin is a cone-type pigment from this point of view, the time constant for the formation of the meta II intermediate of pinopsin was compared with those of rhodopsin and green. The thermal reaction of photoactivated pinopsin was recorded by time-resolved spectroscopy at  $-25^{\circ}\text{C}$  (Figure 5). After the irradiation, the absorbance at 380 nm increased while that at 460 nm decreased (Figure 5A), representing the conversion of metapinopsin I to metapinopsin II. The kinetic profile at 380 nm (Figure 5B, closed circles) was simulated by a single-exponential curve, from which the time constant of metapinopsin II formation was estimated to be 6.2 min. This rate was comparable to that of meta II formation of green (time constant, 2.7 min; Figure 5B), and much faster than that of rhodopsin (time constant, 130 min; Figure 5B). Thus, we concluded that the formation of the meta II intermediate of pinopsin is as fast as those of cone pigments.

**Transducin Activation by Pinopsin.** Similarity in the photobleaching process between pinopsin and the visual pigment, together with the presence of transducin-like G-protein in the chicken pineal gland (34), raised the possibility that pinopsin can activate transducin. As shown in Figure 6, pinopsin activated bovine retinal transducin in a light-dependent manner, and the activation efficiency of pinopsin was comparable to that of rhodopsin. To see whether metapinopsin II is responsible for the activation, we measured the decay time course of the activation ability at  $2^{\circ}\text{C}$  (closed circles; Figure 7A), and compared it with the spectral change at the same temperature (open circles, Figure 7A). In the thermal reaction of photoactivated pinopsin at  $2^{\circ}\text{C}$  (Figure 7B), the absorbance at  $\sim 380\text{ nm}$  decreased with concomitant increase in the absorbance at  $\sim 450\text{ nm}$ , representing the conversion process of metapinopsin II to metapinopsin III. This decay process of metapinopsin II

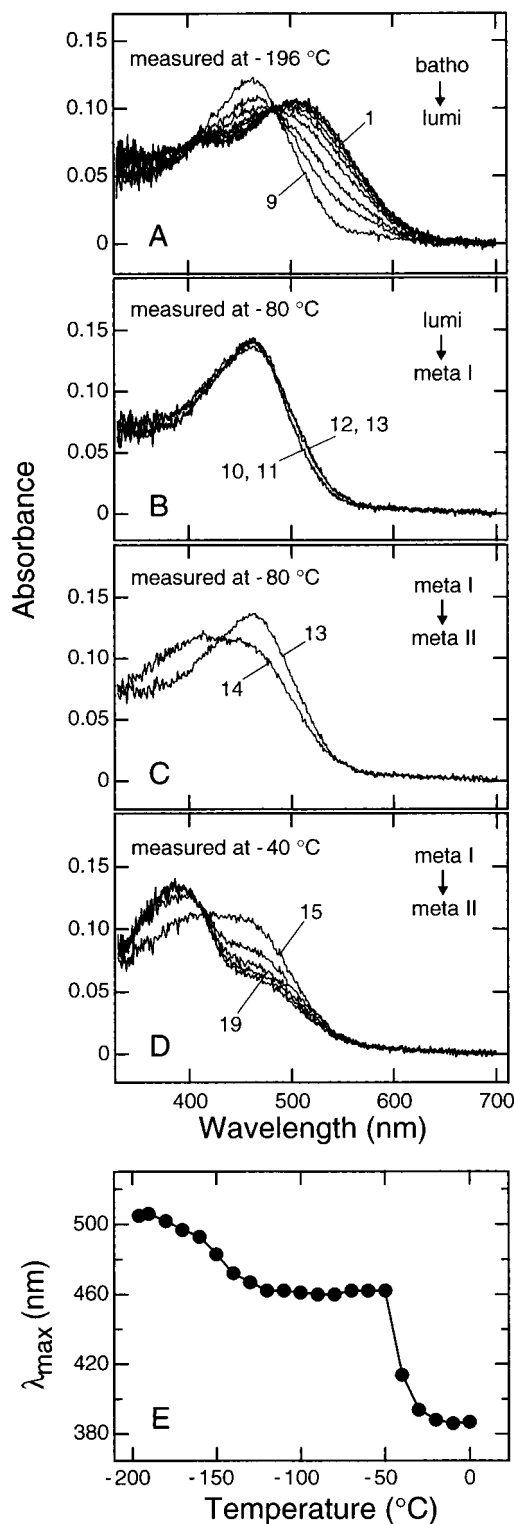


FIGURE 4: Photobleaching process of pinopsin. The photo-steady-state mixture containing mainly batho intermediate formed at  $-196^{\circ}\text{C}$  (curve 1) was warmed in a stepwise manner. (Panel A) Absorption spectra were recorded at  $-196^{\circ}\text{C}$  after warming to  $-190$ ,  $-180$ ,  $-170$ ,  $-160$ ,  $-150$ ,  $-140$ ,  $-130$ , and  $-120^{\circ}\text{C}$  (curves 2–9). (Panel B) Absorption spectra were recorded at  $-80^{\circ}\text{C}$  after warming to  $-190$ ,  $-180$ ,  $-170$ ,  $-160$ ,  $-150$ ,  $-140$ ,  $-130$ , and  $-120^{\circ}\text{C}$  (curves 10–13). (Panel C) Absorption spectra were recorded at  $-80^{\circ}\text{C}$  after warming to  $-40^{\circ}\text{C}$  (curve 14). (Panel D) Absorption spectra were recorded at  $-40^{\circ}\text{C}$  after warming to  $-40$ ,  $-30$ ,  $-20$ ,  $-10$ , and  $0^{\circ}\text{C}$  (curves 15–19). (Panel E) Absolute  $\lambda_{\text{max}}$  values of the recorded spectra were plotted against the temperatures to which the sample was warmed.

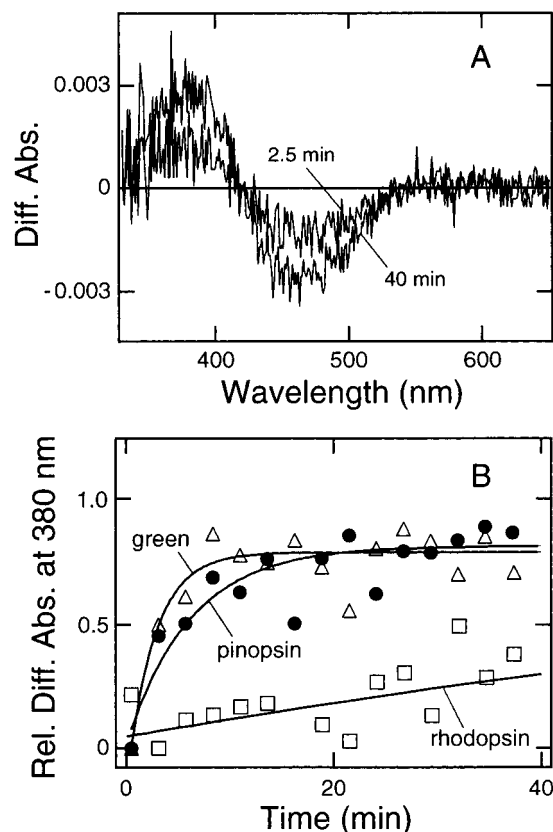


FIGURE 5: Formation of meta II intermediate of pinopsin at  $-25^{\circ}\text{C}$ . (Panel A) Purified pinopsin in a 67% (v/v) glycerol mixture was cooled to  $-25^{\circ}\text{C}$ , and irradiated with orange light ( $>520\text{ nm}$ ) for 30 s. After the irradiation, the sample was incubated in the dark at the same temperature. The curves were the difference spectra between the spectrum recorded immediately after irradiation and those recorded 2.5 and 40 min after the irradiation. (Panel B) The kinetic profiles of the meta II formation of pinopsin (closed circles) were compared with those of rhodopsin (open squares) and green (open triangles). Relative absorbance changes at 380 nm after the irradiation were plotted against incubation time after the irradiation. The irradiation of rhodopsin and green was performed with orange light ( $>570\text{ nm}$ ) for 30 s. Solid curves represent single-exponential curves fitted with time constants of 6.2 min (pinopsin), 2.7 min (green), and 130 min (rhodopsin), respectively.

(reproduced in Figure 7A, open circles) was nearly identical to the decay of the active state, though the calculated time constant for the latter ( $69 \pm 11\text{ min}$ ) was slightly larger than that for the former (44 min). Such a small difference could be due to the existence of the equilibrium between metapinopsin II and metapinopsin III (35), and thus we assigned metapinopsin II as an important intermediate activating transducin.

**Decay Processes of Metapinopsin II, Metarhodopsin II, and Meta-green II.** The lifetime of metapinopsin II was compared with those of green and rhodopsin. As described above, the decay of metapinopsin II at  $2^{\circ}\text{C}$  was a relatively slow process with a time constant of 44 min estimated from the kinetic profile at 470 nm (Figure 7C, open circles). This decay time constant was comparable to that of metarhodopsin II (91 min; Figure 7C, open squares). Under the same conditions, the decay of the meta II intermediate of green was not detected, and instead the decay process of meta III was observed (Figure 7C, closed triangles), indicating that the decay of meta-green II was completed within 0.5 min. Thus, the decay time constant for metapinopsin II (44 min)

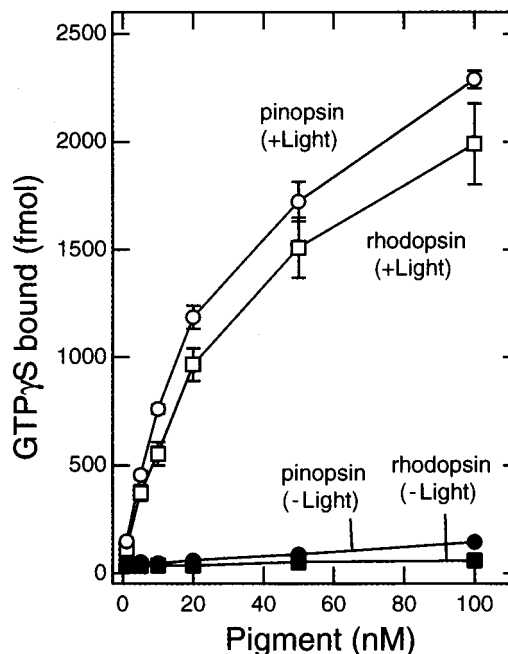


FIGURE 6: Light-dependent activation of transducin by pinopsin and rhodopsin. Pinopsin or rhodopsin at various concentrations (final concentrations are indicated on the abscissa) was mixed with 500 nM bovine transducin and  $3\text{ }\mu\text{M}$  [ $^{35}\text{S}$ ]GTP $\gamma\text{S}$  in 0.01% DM (final concentrations). Reactions proceeded under irradiation (pinopsin,  $>480\text{ nm}$ ; rhodopsin,  $>520\text{ nm}$ ) for 30 s and subsequently in the dark for 30 s at  $2^{\circ}\text{C}$ , and then the amount of GTP $\gamma\text{S}$  bound to transducin  $\alpha$ -subunit was measured. Average values and standard deviations from three independent experiments are presented.

is rather similar to that of metarhodopsin II (91 min), but much larger (at least 80 times) than that of meta-green II.

## DISCUSSION

Using recombinant pinopsin, we investigated for the first time the photobleaching process of such an extra-retinal pigment in detail by low-temperature spectroscopy. When a retinal visual pigment such as rhodopsin is exposed to blue light at  $-196^{\circ}\text{C}$ , the batho intermediate is observed as the primary photoproduct with a twisted all-*trans* chromophore (5). This intermediate is converted to iso-product with the 9-*cis* chromophore upon exposure to red light at  $-196^{\circ}\text{C}$ . That is, light induces only geometric isomerization of the chromophore at  $-196^{\circ}\text{C}$ , leaving the protein moiety relatively unaltered (5). In the present study, quite similar photoreversibility was observed among pinopsin, bathopinopsin, and isopinopsin (Figure 3), strongly suggesting that the 11-*cis*-retinylidene chromophore of pinopsin is isomerized to the all-*trans* form by light. This seems to be supported by the occurrence of 11-*cis*- and all-*trans*-retinal in the chicken pineal gland (36, 37), though the chromophore analysis of native pinopsin has not been performed due to the low content in a single pineal gland (approximately 2 ng; ref 24).

In the photobleaching process of pinopsin, we detected several intermediates, each of which spectrophotometrically corresponds to that of a retinal visual pigment. As shown in Figure 8, the  $\lambda_{\text{max}}$ 's of meta I, meta II, and meta III of pinopsin respectively converge to those of visual pigments, while batho and lumi intermediates of these pigments have

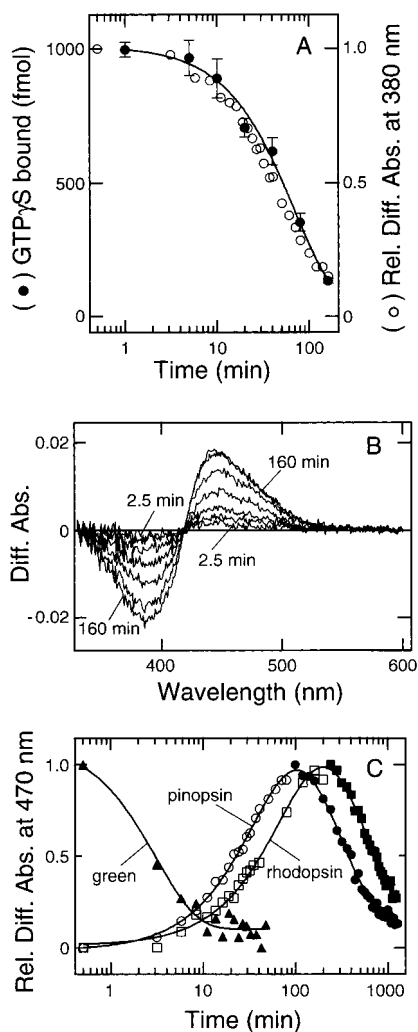


FIGURE 7: Thermal decay of the meta II intermediate of pinopsin at 2 °C. (Panel A) The mixture of pinopsin and [ $^{35}$ S]GTP $\gamma$ S was irradiated at 2 °C with yellow light (>480 nm) for 30 s. After incubation for the indicated time (abscissa) in the dark at 2 °C, 15  $\mu$ L aliquots were withdrawn and mixed with 5  $\mu$ L of transducin solution (final concentrations: 15 nM pinopsin, 500 nM transducin, 3  $\mu$ M [ $^{35}$ S]GTP $\gamma$ S) for measurement of the GTP $\gamma$ S binding activity. Average values (closed circles) with standard deviations from three independent experiments were fitted with a single-exponential curve with a time constant of  $69 \pm 11$  min. The thermal decay of metapinopsin II at 2 °C (open circles) was assessed by the decrease in absorbance at 380 nm (see below). (Panel B) Pinopsin was irradiated with yellow light (>480 nm) at 2 °C for 30 s, and the sample was subsequently incubated in the dark at the same temperature. The curves were the difference spectra between the spectrum recorded immediately after irradiation and those recorded 2.5, 5, 10, 20, 40, 80, and 160 min after the irradiation. (Panel C) The thermal conversion of meta intermediates of pinopsin (circles), rhodopsin (squares), or green (triangles) was assessed by relative absorbance changes at 470 nm plotted against incubation time after irradiation. Rhodopsin or green was irradiated with orange light (>520 nm) at 2 °C for 30 s. The absorbance changes of pinopsin and rhodopsin were simulated by a combination of two sequential single-exponential curves. The first phase of each curve represents the formation of meta III from meta II, i.e., meta II decay (open symbols), and the second phase represents the decay of meta III (closed symbols). The calculated time constants for the first phase of pinopsin and rhodopsin are 44 and 91 min, respectively, and those for the second phase are 320 and 590 min, respectively. As for green, only the decay of meta III (closed triangles) was observed (time constant, 3.9 min) due to a rapid conversion of meta II to meta III intermediates at this temperature.

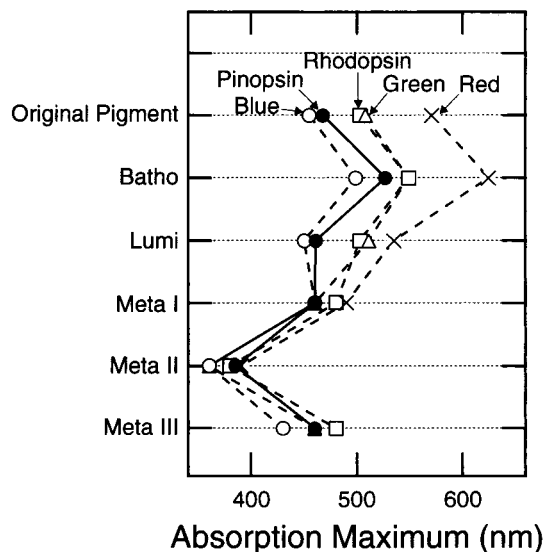


FIGURE 8: Shift of absorption maxima of the intermediates appearing in the photobleaching process of pinopsin and chicken visual pigments. Plotted are the absorption maxima of the intermediates of pinopsin (closed circles), rhodopsin (open squares), green (open triangles), blue (open circles), and red (crosses), among which those of rhodopsin, red, green, and blue are reproduced from previous reports (9, 11, 31, 32, 41, 42).

their unique  $\lambda_{\max}$ 's. This suggests that the chromophore/opsin interactions and opsin conformations of meta I, II, and III of pinopsin are respectively similar to the corresponding intermediates of visual pigments. Judging from the  $\lambda_{\max}$  profile, we speculate that the conformational change of pinopsin after photon absorption resembles those of rod and cone visual pigments, among which chicken blue seems most similar to pinopsin in overall structural change (Figure 8).

The present result demonstrated that chicken pinopsin activates transducin in a light-dependent manner. Recently, transducin activation by pinopsin has been reported by Max et al. (38), but their data are somewhat different from ours in two aspects. First, the lifetime of the active state of pinopsin is about 2 times longer than that of rhodopsin purified from bovine retinas (38), but the present data (Figure 7C) show that the lifetime of metapinopsin II is about half of that of metarhodopsin II derived from histidine-tagged recombinant rhodopsin. Second, the initial rate of transducin activation by pinopsin is 2–3 times lower than that by retinal rhodopsin in their report (38), while we observed that pinopsin can activate transducin with an initial rate comparable to that of recombinant rhodopsin upon exposure to light (Figure 6). Such disagreements might come from a difference in the preparation of pinopsin (and rhodopsin). Max et al. (38) used recombinant pinopsin with a 1D4 epitope tag added to the C-terminus. Transducin activation by pinopsin may be perturbed due to the tagging to the C-terminal tail, which is located at the molecular surface interacting with G-protein. To avoid such a possible perturbation, we introduced a histidine tag to the N-terminus located at the extracellular surface. In addition, we prepared recombinant rhodopsin having the same histidine-tag at the N-terminus to minimize or cancel out a possible artificial effect of the tagging on the evaluation of the functional difference between pinopsin and rhodopsin. Our preparation would help detailed characterization of the unidentified functional importance of the pinopsin C-terminal tail, of which the amino acid sequence

is noticeably diverged from those of rod and cone visual pigments (6).

The present results demonstrated that the decay of metapinopsin II is relatively slow (rod-type), while its formation is relatively rapid (cone-type). The rod-type decay process of metapinopsin II was unexpected, because pinopsin was predicted to be a cone-type pigment on the basis of the following three reasons: First, like cone pigments, pinopsin has an isoelectric point much more basic than rhodopsins (6), and the difference in isoelectric point between cone pigments and rhodopsins is one of the important factors regulating the thermal behaviors of the meta II intermediate (9). Second, a phylogenetic tree of vertebrate pigments indicated that pinopsin has diverged from an ancestor of cone pigments before the divergence of rhodopsins from cone pigments (6). Third, chicken pinopsin as well as most of the cone visual pigments has a neutral amino acid residue at position 122 (a number in chicken rhodopsin), while all the sequenced rhodopsins have a glutamate at this position. This single amino acid residue is a major determinant of the meta II decay rate of rod and cone pigments (10). Despite these cone-type features of pinopsin, we found a long-lived metapinopsin II, suggesting an unidentified regulatory mechanism of the meta II lifetime unique to pinopsin.

What is the physiological significance of the relatively long lifetime of metapinopsin II? A simple speculation is that pinopsin might adapt to detecting changes in the environmental light conditions by stabilizing its active state for mediating circadian photoregulation in the pineal gland. The cellular structure of the pinealocytes may suggest another role of the thermal stability of metapinopsin II: The outer segment of the retinal photoreceptor cell is a specialized unit composed of a highly stacked multilamellar structure capable of detecting light effectively. On the other hand, the outer segments of avian pinealocytes are generally degenerated without regular structures (23, 39). Thus, it is likely that pinopsin acquired the long-lived active state to effectively activate G-protein (and/or other signaling molecules) at the expense of time resolution. In addition to the long lifetime of metapinopsin II, a reduced number of phosphorylation sites in the pinopsin C-terminal tail (6) might also be important in extending activation of the phototransduction cascade. Alternatively, the long-lived active state of pinopsin might be favorable to interact with another type of G-protein in addition to transducin. In chicken pinealocytes, light causes two distinct effects; one is the acute suppression of melatonin synthesis, and the other is the phase-shifting of the circadian rhythm of melatonin synthesis (4, 40). The acute light-signaling pathway is sensitive to pertussis toxin-treatment, whereas the phase-shifting pathway is insensitive (4, 40). The long lifetime of metapinopsin II might be required to trigger the two pathways simultaneously or with a time delay by activating both transducin and a certain pertussis toxin-insensitive G-protein such as  $G_{\alpha}$  (38).

The purified preparation of recombinant pinopsin with an intact C-terminal tail enables us to assess the exact nature of the interaction of pinopsin with other signaling molecules such as G-protein-coupled receptor kinase, arrestin, or other unidentified molecules in future studies. Such an analysis is required to unravel pineal-specific photon-signaling mechanisms including a possible photo-regulation of the endogenous circadian pacemaker in the chicken pineal gland.

## ACKNOWLEDGMENT

We thank Prof. J. Nathans for providing pRSV-Tag, and 293S cells. We also thank Dr. K. Sanada, Dr. T. Yoshikawa, Ms. F. Shimizu, and Mr. Y. Hashimoto for valuable discussions, Mr. T. Yamashita for technical advice about the GTP $\gamma$ S binding assay and for helpful discussions, and Dr. T. Matsuda for the preparation of bovine rod transducin.

## REFERENCES

1. Deguchi, T. (1979) *Science* 203, 1245–1247.
2. Deguchi, T. (1981) *Nature* 290, 706–707.
3. Zatz, M., Mullen, D. A., and Moskal, J. R. (1988) *Brain Res.* 438, 199–215.
4. Takahashi, J. S., Murakami, N., Nikaido, S. S., Pratt, B. L., and Robertson, L. M. (1989) *Recent Prog. Horm. Res.* 45, 279–352.
5. Shichida, Y., and Imai, H. (1998) *Cell. Mol. Life Sci.* 54, 1299–1315.
6. Okano, T., Yoshizawa, T., and Fukada, Y. (1994) *Nature* 372, 94–97.
7. Shichida, Y., Imai, H., Imamoto, Y., Fukada, Y., and Yoshizawa, T. (1994) *Biochemistry* 33, 9040–9044.
8. Okada, T., Matsuda, T., Kandori, H., Fukada, Y., Yoshizawa, T., and Shichida, Y. (1994) *Biochemistry* 33, 4940–4946.
9. Imai, H., Imamoto, Y., Yoshizawa, T., and Shichida, Y. (1995) *Biochemistry* 34, 10525–10531.
10. Imai, H., Kojima, D., Oura, T., Tachibanaki, S., Terakita, A., and Shichida, Y. (1997) *Proc. Natl. Acad. Sci. U.S.A.* 94, 2322–2326.
11. Imai, H., Terakita, A., Tachibanaki, S., Imamoto, Y., Yoshizawa, T., and Shichida, Y. (1997) *Biochemistry* 36, 12773–12779.
12. Fukada, Y., and Yoshizawa, T. (1981) *Biochim. Biophys. Acta* 675, 195–200.
13. Emeis, D., and Hofmann, K. P. (1981) *FEBS Lett.* 136, 201–207.
14. Bennett, N., Michel-Villaz, M., and Kühn, H. (1982) *Eur. J. Biochem.* 127, 97–103.
15. Okano, T., Kojima, D., Fukada, Y., Shichida, Y., and Yoshizawa, T. (1992) *Proc. Natl. Acad. Sci. U.S.A.* 89, 5932–5936.
16. Kayada, S., Hisatomi, O., and Tokunaga, F. (1995) *Comp. Biochem. Physiol.* 110B, 599–604.
17. Shimamoto, A., Kimura, T., Matsumoto, K., and Nakamura, T. (1993) *FEBS Lett.* 333, 61–66.
18. Nathans, J., Weitz, C. J., Agarwal, N., Nir, I., and Papermaster, D. S. (1989) *Vision Res.* 29, 907–914.
19. Gorman, C. M., Gies, D. R., and McCray, G. (1990) *DNA Protein Eng. Tech.* 2, 3–10.
20. Maeda, A., Shichida, Y., and Yoshizawa, T. (1978) *J. Biochem.* 83, 661–663.
21. Fukada, Y., Matsuda, T., Kokame, K., Takao, T., Shimonishi, Y., Akino, T., and Yoshizawa, T. (1994) *J. Biol. Chem.* 269, 5163–5170.
22. Terakita, A., Yamashita, T., Tachibanaki, S., and Shichida, Y. (1998) *FEBS Lett.* 439, 110–114.
23. Okano, T., Takanaka, Y., Nakamura, A., Hirunagi, K., Adachi, A., Ebihara, S., and Fukada, Y. (1997) *Mol. Brain Res.* 50, 190–196.
24. Takanaka, Y., Okano, T., Iigo, M., and Fukada, Y. (1998) *J. Neurochem.* 70, 908–913.
25. Okano, T., Fukada, Y., Artamonov, I. D., and Yoshizawa, T. (1989) *Biochemistry* 28, 8848–8856.
26. Yoshizawa, T., and Wald, G. (1963) *Nature* 197, 1279–1286.
27. Yoshizawa, T., and Wald, G. (1967) *Nature* 214, 566–571.
28. Imamoto, Y., Kandori, H., Okano, T., Fukada, Y., Shichida, Y., and Yoshizawa, T. (1989) *Biochemistry* 28, 9412–9416.
29. Kojima, D., Imai, H., Okano, T., Fukada, Y., Crescitelli, F., Yoshizawa, T., and Shichida, Y. (1995) *Biochemistry* 34, 1096–1106.
30. Matthews, R. G., Hubbard, R., Brown, P. K., and Wald, G. (1963) *J. Gen. Physiol.* 47, 215–240.

31. Shichida, Y., Okada, T., Kandori, H., Fukada, Y., and Yoshizawa, T. (1993) *Biochemistry* 32, 10832–10838.
32. Imai, H., Mizukami, T., Imamoto, Y., and Shichida, Y. (1994) *Biochemistry* 33, 14351–14358.
33. Yoshizawa, T., and Shichida, Y. (1982) *Methods Enzymol.* 81, 333–354.
34. Okano, T., Yamazaki, K., Kasahara, T., and Fukada, Y. (1997) *J. Mol. Evol.* 44, 91–97.
35. Kibelbek, J., Mitchell, D. C., Beach, J. M., and Litman, B. J. (1991) *Biochemistry* 30, 6761–6768.
36. Sun, J.-H., Reiter, R. J., Mata, N. L., and Tsin, A. T. C. (1991) *Neurosci. Lett.* 133, 97–99.
37. Masuda, H., Oishi, T., Ohtani, M., Michinomae, M., Fukada, Y., Shichida, Y., and Yoshizawa, T. (1994) *Tissue Cell* 26, 101–113.
38. Max, M., Surya, A., Takahashi, J. S., Margolskee, R. F., and Knox, B. E. (1998) *J. Biol. Chem.* 273, 26820–26826.
39. Ohshima, K., and Matsuo, S. (1991) *Anat. Anz. Jena* 172, 247–255.
40. Zatz, M., and Mullen, D. A. (1988) *Brain Res.* 453, 63–71.
41. Fukada, Y., Okano, T., Shichida, Y., Yoshizawa, T., Trehan, A., Mead, D., Denny, M., Asato, A. E., and Liu, R. S. H. (1990) *Biochemistry* 29, 3133–3140.
42. Kandori, H., Mizukami, T., Okada, T., Imamoto, Y., Fukada, Y., Shichida, Y., and Yoshizawa, T. (1990) *Proc. Natl. Acad. Sci. U.S.A.* 87, 8908–8912.

BI9913496